Bull. Min. Res. Exp. (2022) 167: 189-207

Bulletin of the Mineral Research and Exploration

http://bulletin.mta.gov.tr

A walkaway vertical seismic profiling modeling and imaging study and combining its results with migrated surface seismic images

Cemal ERDEMİR[a*]

[a]*Geophysical Consultant, Houston, Texas, USA*

Research Article

Keywords:
Walkaway Vertical Seismic Profiling, Finite Difference Modeling, Reverse Time Migration, Imaging, Seismic.

Received Date: 17.12.2020
Accepted Date: 10.08.2021

ABSTRACT

This paper presents and analyzes results from a Finite Difference Modeling (FDM), processing, and imaging study of a Walkaway Vertical Seismic Profiling (WVSP) survey, and discusses how the images from WVSP enhance those from the surface seismic data. It is shown that the results from the WVSP integrate well with the image from the surface seismic performed in the same line. For the study, a seismic model with vertically and horizontally varying velocities was built and a WVSP data set was generated. The surface seismic had difficulty showing clear images from the layers with steep dips and near vertical displacements on the model due to the lack of ray coverage. The study demonstrates that the WVSP geometry can record reflections from near vertical layers facing the borehole, which help with imaging the parts of the subsurface structure which were missing in the surface seismic. With the proper combination of the images from the WVSP and the surface seismic, a more complete image profile of the subsurface can be constructed around the borehole. However, while contributing to surface seismic, it is also seen that the WVSP introduces more migration artifacts related to source interval distance and interbed multiples than the surface seismic data.

1. Introduction

When a surface seismic survey is conducted, it is desirable that all geologic layers in the subsurface are imaged properly and in their correct locations. Given appropriate acquisition parameters and source-receiver geometry, a seismic survey provides key, targeted information regarding the geological structure in a survey area. However, in order to image the desired subsurface layers of interest, it is obviously a prerequisite that seismic reflections be recorded for those layers. Hence, careful consideration of the dips of the layers is important for the successful imaging of all reflectors under the constraints of a particular acquisition geometry. Steep dips may require long source-receiver offsets to capture their reflections, and in extreme cases, where dips are approaching 90 degrees, reflections from such surfaces may not even be recorded using surface seismic geometry. Under these circumstances, a vertical seismic profiling (VSP) method gains importance for consideration. In a VSP survey, the seismic sources are located at the surface and the receivers are at multiple depth levels in a well. With this geometry reflection from steeply dipping surfaces or vertical layers can be captured by the subsurface receivers before they scatter away into the medium, and away from the receivers of the surface seismic survey geometry. This phenomenon is the subject of this paper.

Citation Info: Erdemir, C. 2022. A walkaway vertical seismic profiling modeling and imaging study and combining its results with migrated surface seismic images. Bulletin of the Mineral Research and Exploration 167, 189-207.
https://doi.org/10.19111/bulletinofmre.981941

Corresponding author: Cemal ERDEMİR, cerdemir_2000@yahoo.com

WVSP modeling and imaging studies have been widely used in seismic exploration (Balch and Lee, 1984; Galperin, 1985; Hardage, 1985; Toksöz and Stewart, 1985; Wyatt, 1987; Yılmaz, 1987), especially for survey design before performing a field survey (Jaramillo, 1993; Ray et al., 2005; Hornby et al., 2006). Erdemir (2018) demonstrated on a surface seismic model that a vertical layer and a steeply dipping reflector was not able to be imaged with that acquisition geometry. A WVSP survey was proposed on the same line to see if the missing parts in the surface seismic could be recovered. For this purpose, a synthetic data set is generated using an FDM method for the WVSP survey. The data set is processed, imaged and compared to the surface seismic in this study. Its results are presented in the following sections.

2. The Problem

The problem can be stated: Can geological structures with steeply dipping layers or vertical faults be imaged using a WVSP geometry? This question has especially importance in areas where those layers cannot be clearly imaged using a standard surface seismic geometry. The final image and its comparison with the model reproduced here from the earlier study (Erdemir, 2018) and shown in Figure 1a and Figure 1b respectively, form the basis for this study. The figure shows that the accuracy of the images and the continuity of the layers are quite good, and the undulating middle layer is nicely focused. However, while the flat areas of the bottom layer are imaged well, the zones indicated by the arrows are not imaged clearly, the vertical zone on the left looks like a right dipping layer and the steeply dipping layer on the right is missing.

In order to capture the reflections from those sides, a WVSP survey with a borehole located in the middle of the model is designed as shown in Figure 2 where some straight, conceptual reflection ray paths annotated, S represents the source. Reflections from the steeply dipping structures are expected to be imaged by the WVSP, as shown in (Jaramillo, 1993).

3. Forward Modeling and the Synthetic Data Set

The forward modeling is accomplished using a second-order finite difference algorithm from the SU package (Stockwell and Cohen, 2008). A constant

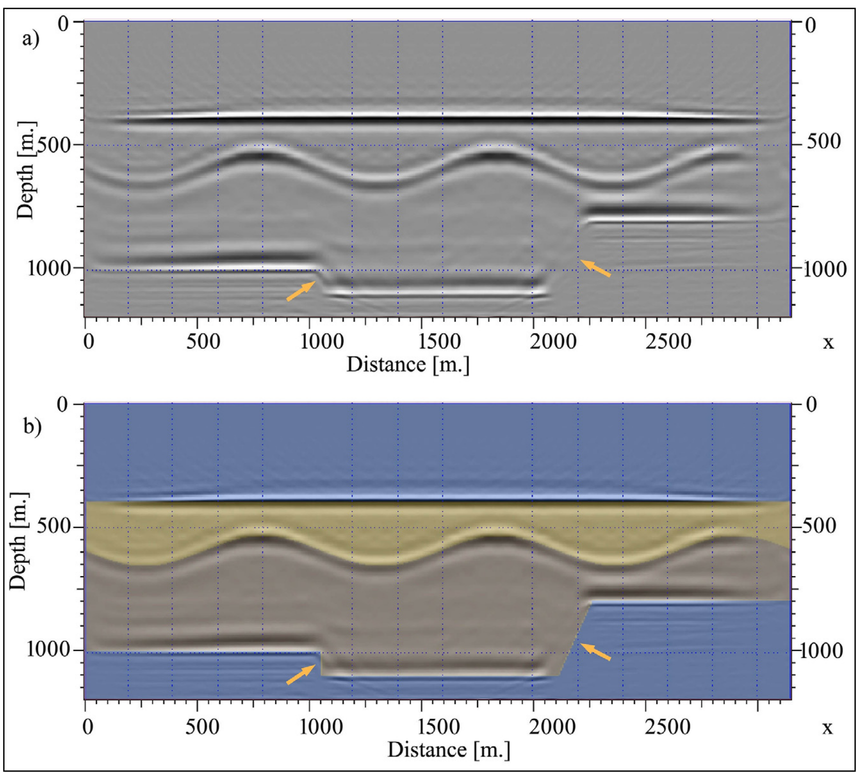

Figure 1- a) Stacked image from the surface seismic data, b) the image is compared with the model. Arrows show the places that are not imaged well (Erdemir, 2018).

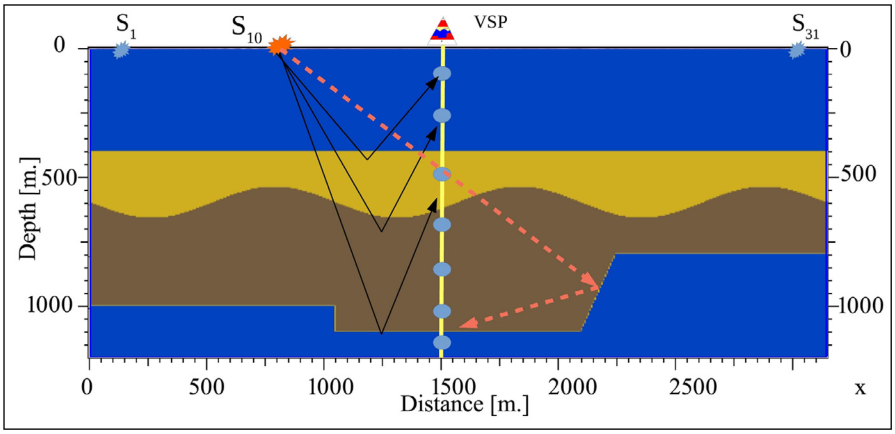

Figure 2- Proposed WVSP survey, schematic display. Expected potential reflections are shown by the dashed line.

density is assumed in the model for simplicity. The velocity contrasts in the model define the four structural layers, as shown in Figure 2. Velocities are constant within the layers. Absorbing boundary conditions are used in the modeling on four sides of the model. Surface multiples are therefore suppressed, and only the reflections originating within the model are recorded. The same source is used for both WVSP and the surface seismic data sets. The source waveform used in the modeling is shown in Figure 3 where the waveform is repeated five times for clarity. The data was generated with 50 Hz maximum and 25 Hz dominant frequency. The modeling grid size was 5 m in both x and z.

There are 31 shots placed at 10 m depth below the surface of the model and 240 receivers located in the borehole for the WVSP geometry. Shot spacing was

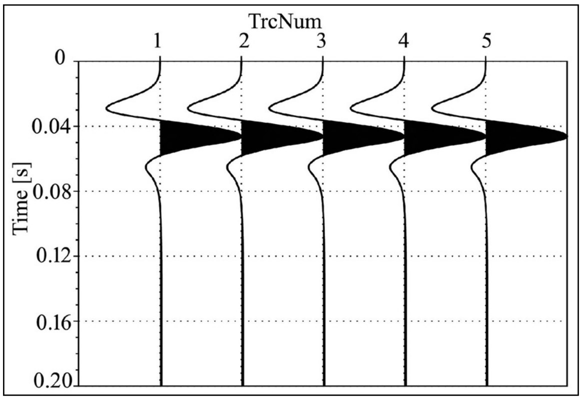

Figure 3- Seismic waveform used in the FDM to create the WVSP data. It is repeated five times (https://gpg.geosci.xyz/content/physical_20properties/seismic_velocity_duplicate.html)..

100 m. and receiver interval 5 m. For source location 15 (S_{15}), which corresponds to x=1500 m, the model, the surface gather, the VSP gather in depth-oriented format and the VSP gather in time-oriented standard format are shown together in Figure 4. The VSP borehole is at x=1550 m. The reflections in the depth-oriented section match the depths of the layers on the model, whereas the VSP gather matches the surface seismic gather in the time-oriented section. As seen in the figure, the VSP serves as a bridge between the subsurface and surface seismic and is a direct way to tie surface seismic to subsurface structures in depth.

4. WVSP Data Processing

The VSP data processing was completed using several software packages, including SU, FreeUSP/FreeDDS, and an imaging package which was developed at Colorado School of Mines (CSM), Geophysics Department. The VSP processing was done both in common shot gather (CSG) and common receiver gather (CRG) domains. The data were transferred between the domains, back and forth, for quality control (QC) and analysis of the processing steps which began with data display and first break picking and concluded with pre-stack common shot gather migrations. Also, a composite image is produced by combining WVSP and surface seismic images. A flow chart for the WVSP processing sequence is constructed and shown in Figure 5.

5. Data Processing Steps and Findings

A selection of the processing steps and their results is presented here for review. A WVSP smashed plot

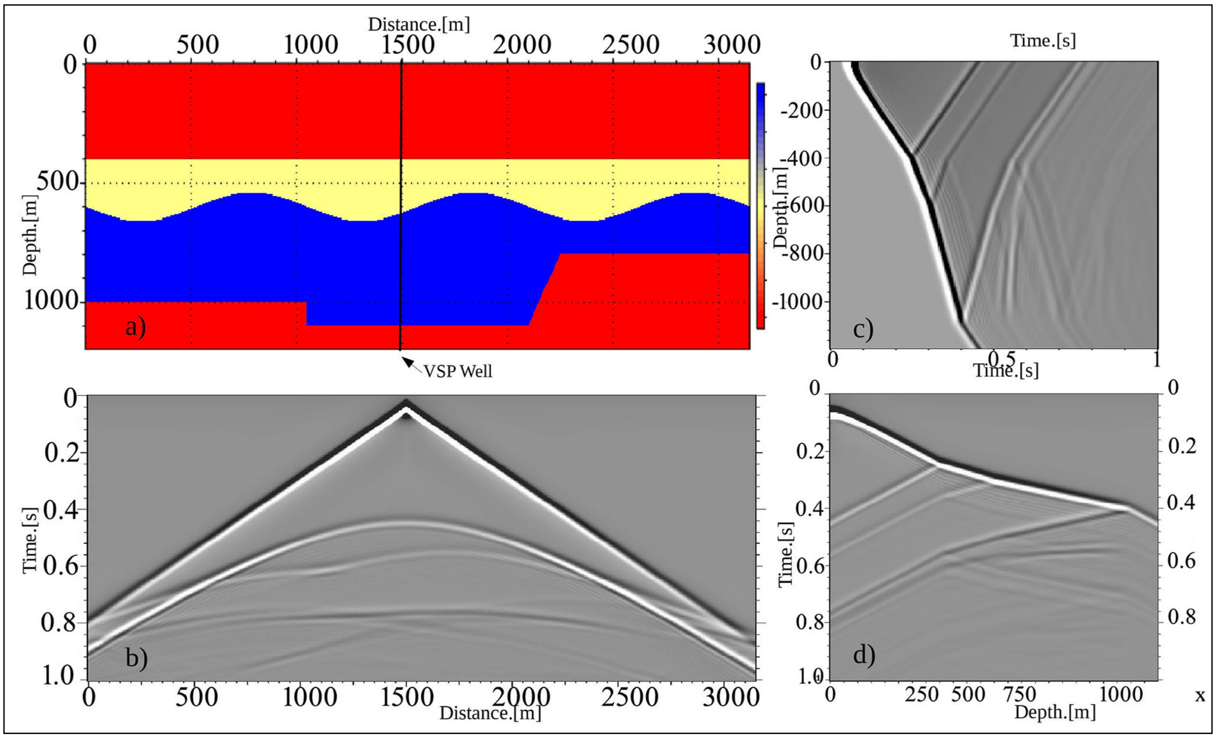

Figure 4- A combined illustration of the modeling; a) the model, b) surface seismic gather at the well location, c) VSP gather as depth-oriented, d) VSP gather in the standard time-oriented display.

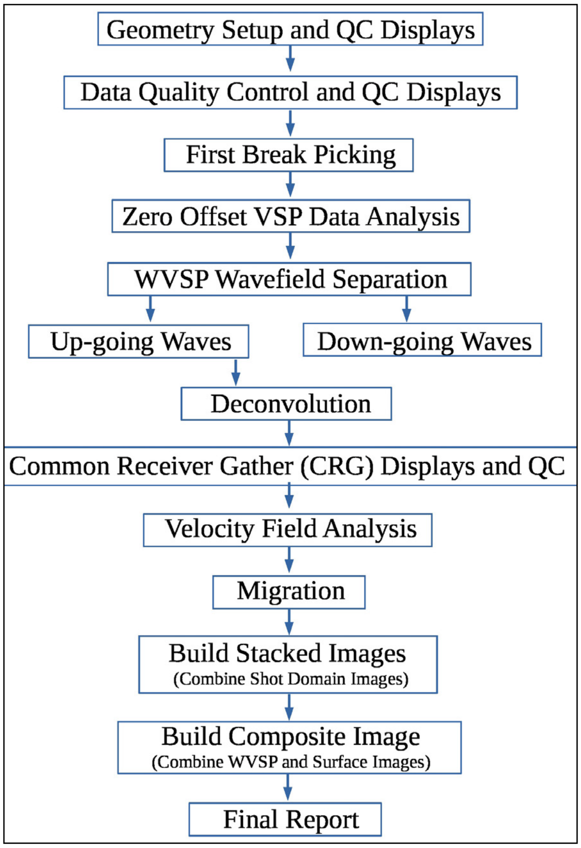

Figure 5- WVSP processing flow chart.

is constructed by combining all the data together and shown in Figure 6. A smash plot is used to view data quality and data geometry quickly and easily. As seen in the figure, no spikes or geometry problems are recognized on the data set.

The relationship between the surface seismic and the VSP shot gathers for shot S_{15} is analyzed and summarized in Figure 7. In the figure, the reflections of the surface seismic gather are analyzed for their depths. The reflections on the surface gather are time matched to the reflections in the VSP data at the borehole location (the green line), and the reflections are followed on the VSP section until they intercept the down going first arrivals. The intercept points correspond to the depths at which the reflections in the surface data are created. They are annotated on the VSP at 400, 600, and 1100 m which are the depths of the layers in the model.

Every other shot gather from the WVSP data is plotted in Figure 8, where the zero-offset gather is indicated with the arrow. It is clear that the shot gathers no longer look like the zero offset gather as the source moves away from the borehole which is due to

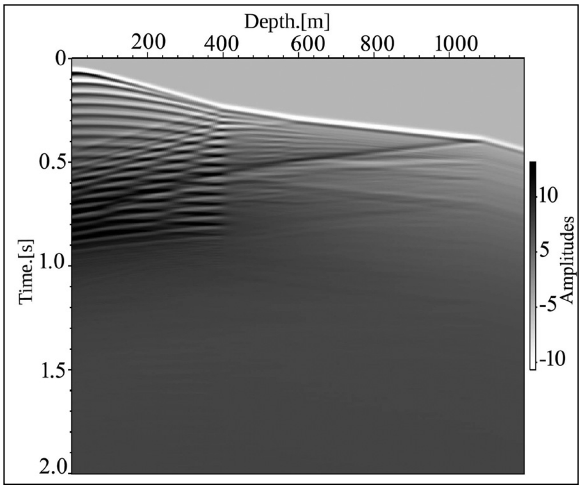

Figure 6- Smashed plot of the WVSP data set.

the increase in the incidence angle from zero to larger angles. At large offsets, strong refractions, caused by the down going waves, contaminate the gathers. The refractions begin interfering with the first breaks on the third gather which is about 600 m away from the zero-offset, indicating that the critical distance (see below) for the interface between the first and second layers has been exceeded.

The maximum source offset in the WVSP is 1500 m to the left and 1600 m to the right of the borehole. It is noticed after examining the gathers that the first arrival waveforms behave strangely and at about 400 m they diminish in amplitude because of the interference of the refractions from the second layer.

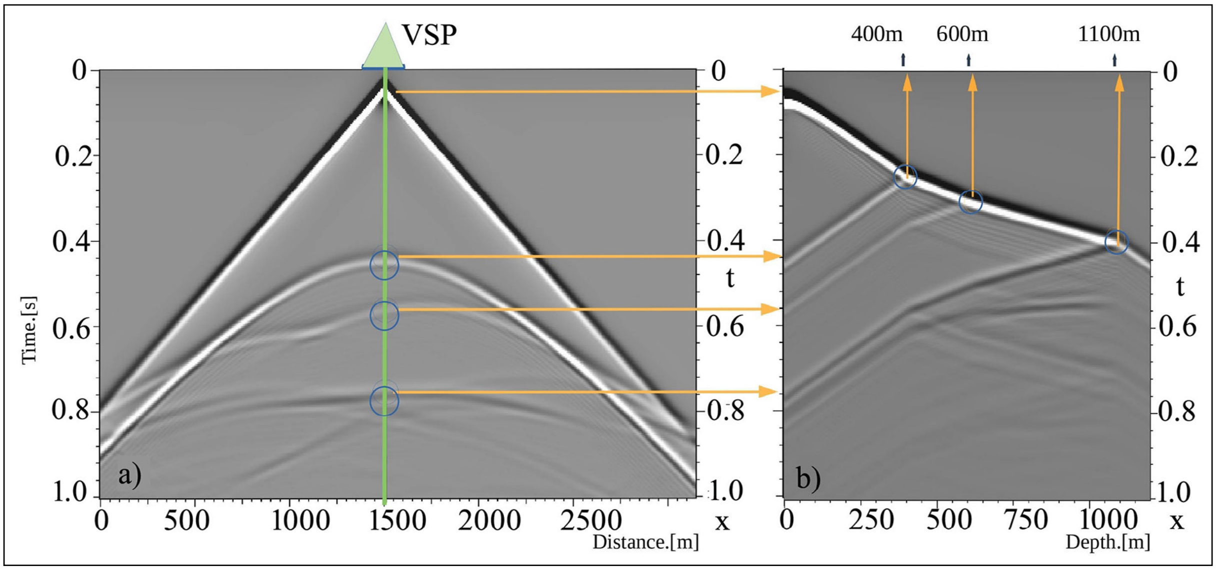

Figure 7- Shot gathers are from the surface shot (S15); a) surface seismic shot gather, b) zero-offset VSP shot gather. The reflections in the surface gather time matched the VSP gather at the borehole location (green line). The depths of the reflections are traced and read in the VSP gather.

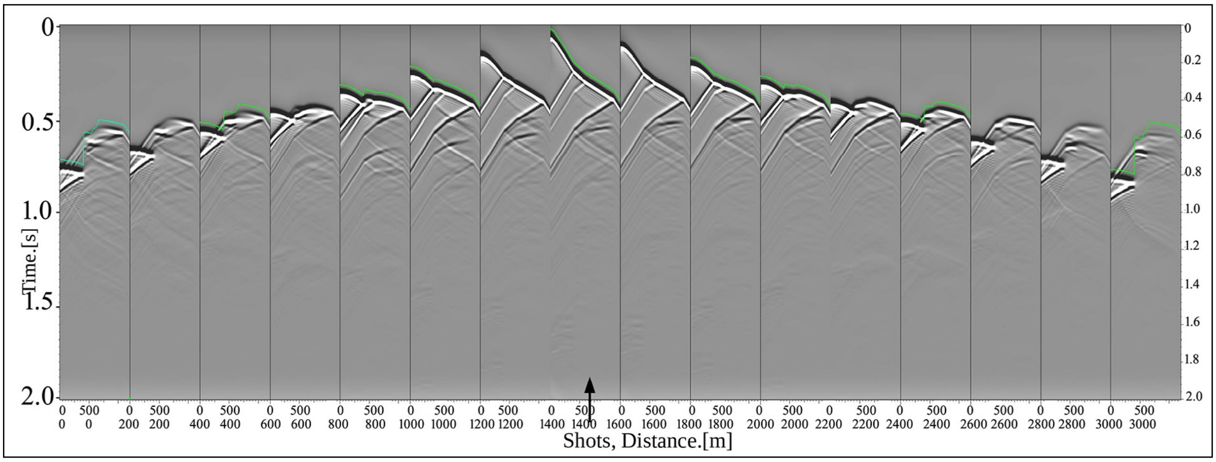

Figure 8- WVSP shot gathers with 200 m shot intervals. The zero offset VSP data is shown by the arrow. The green lines are the calculated first arrival times.

This offset corresponds to the offset distance of the critical ray path and also the critical incident angle between the first and the second layers. On the model, the velocities of the first and second layers are 2000 and 3500 m/s (V_1 and V_2), and the depth to the second layer (H) is 400 m, the critical angle (Θ_c) and the distance (X) between the two layers can be obtained as;

$$\Theta_c = \text{asin}\,(V_1/V_2) \tag{1}$$

$$\Theta_c = \text{asin}\,(2000/3500) = 34.85 \text{ degrees}$$

and

$$X_c = 400 \tan(\theta_c) = 278.5 \text{ m}$$

Where it can be stated that based on the first arrival, the horizontal distance of critical angle is $X_c = H \tan(\theta_c)$.

And for reflection patch, the total source distance for a source and receiver pair at the surface for the reflector of depth H will be

$$X_T = 2 H \tan(\theta_c) \tag{2}$$

Unlike surface seismic, in VSP the depths of the receiver are variant, changing depths results in a different incidence angle for each source-receiver pair yielding changing critical angle (θ_c) at each receiver. Also when the interface has a dip, the formula will change. If more layers are included in the model the procedure for X_T gets complicated, a ray-tracing study is recommended for proper offset values.

Beyond the critical distance (X_c) the down going wave refracts at the interface creating head waves that start to travel horizontally in the second layer towards the receiver. Notice, as V_2 increases the angle Θ_c and distance X_c decrease, and in turn the refraction occurs at a shorter offset distance from the well. The critical distance is an important parameter since it is used to determine where, or at what offsets, the refractions from the second layer will interfere with the reflections from the first layer. The mute zone to remove these degraded reflections can be determined by distance X_c. The refracted energy becomes artifacts on the migrated section creating wide-spread noise events with very high amplitudes. This effect was overwhelmingly observed in this study also. Hence, the refractions were eliminated before migration.

5.1. Examining the Zero-offset VSP Data

The Zero-Offset VSP (ZVSP) gather is quite unique in that it provides a simple way to estimate the formation velocity and seismic wavelet. Since the seismic source is close to the well (50 m in this model) and the receivers are in the borehole, a direct measurement of the source waveforms can be done at each receiver depth, observing the changes in the waveforms as a function of depth can yield information about the subsurface along the borehole. The P-wave first arrival times are picked on the seismic traces and a time-depth pair table is constructed from the picks. The interval velocities (V_i) are calculated from the first break times as follows;

$$V_i = \Delta z_i / \Delta t_i \tag{3}$$

$$\Delta z = z_2 - z_1 \quad \text{difference in depth} \tag{4}$$

$$\Delta t = t_2 - t_1 \quad \text{difference in time} \tag{5}$$

The RMS and the stacking velocities can then be derived from the interval velocities.

The ZVSP gather is examined in Figure 9, as the raw gather on which the first-breaks are picked (green curve), the gather after shifting the traces using the picks and aligning the data at 100 ms, and the gather after cross-correlation to correct for fractional changes in the picks. The final picks are plotted in Figure 10 as time-depth pairs. The slopes of the sections of the curve are the interval velocities. Four sections are recognized on the curve. The depths of the sections are directly read on the horizontal scale as 400, 600, 1000, and 1200 m, which correspond to the layer boundaries on the model. The interval velocities are calculated as 2000, 3500, 5000, and 2000 m/s which correspond to the model velocities.

The ZVSP data could be further processed to create a corridor stack trace from the up going reflections which are used to tie surface seismic reflections to VSP recordings. Also from the down going waves first arrivals could be further studied to map and analyze changes in amplitudes with respect to depths for attenuation or Q calculations and their effects on VSP data (Çınar, 1989; Karslı, 1995; Yılmaz, 2015). A detailed analysis of the amplitudes was not performed in this study.

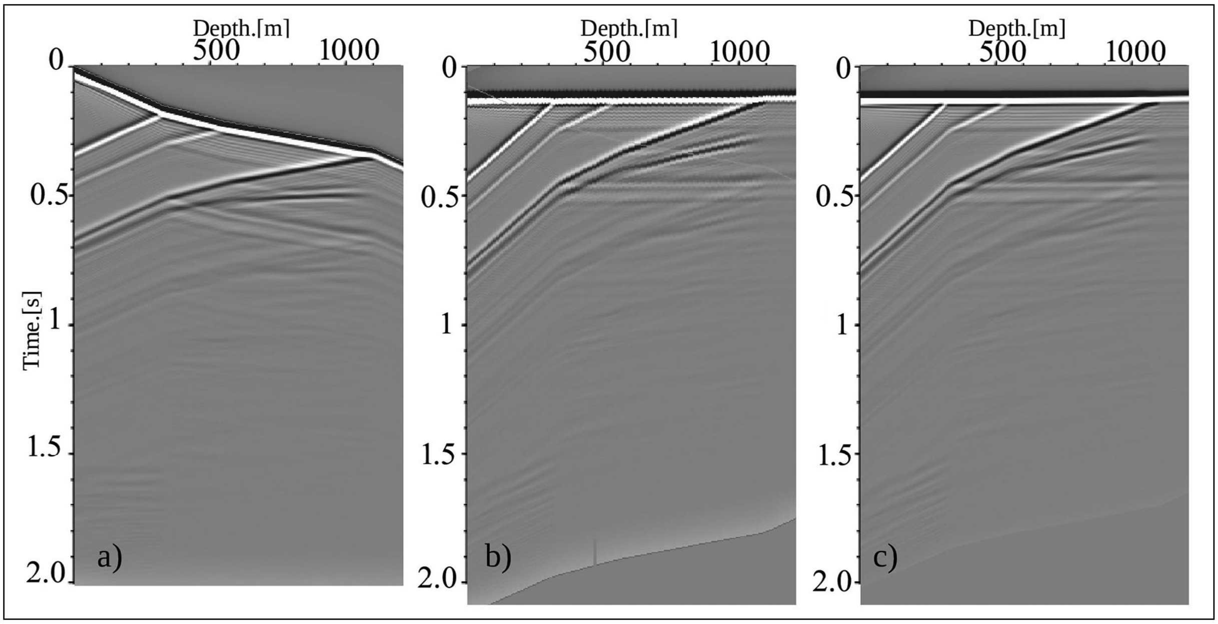

Figure 9- ZVSP shot gather; a) raw data where first breaks are picked, b) the gather is aligned at the first breaks, c) the aligned gather after cross-correlation. The green line is the initial P-wave first breaks picks done on the gather in a.

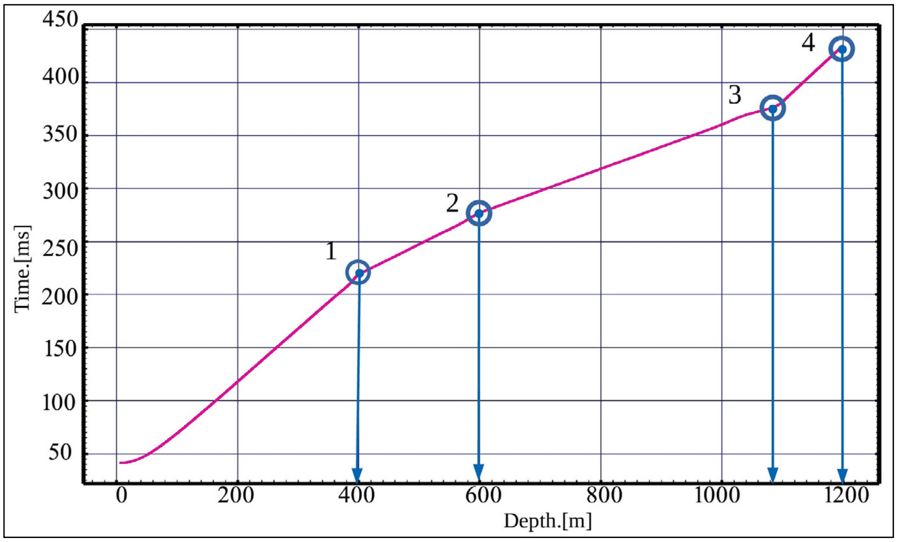

Figure 10- Graph of the first break picks vs. depth. The section boundaries are seen at 400, 600, 1000, 1200 m of depths.

5.2. Wavefield Separation

The wavefield separation processing step separates the up-going waves and down-going waves in a given shot gather. It is an essential step in ZVSP data processing and also can be applied to near offset gathers. Since primary down-going waves travel a shorter distance than do primary reflections, they generally have much stronger amplitudes and usually dominate the VSP gathers, partially obscuring reflection events. Down-going waves are therefore usually removed to reveal up-going reflections.

There are several techniques commonly employed to remove down-going wave fields. One of the most common methods is the frequency-wavenumber (f-k) separation technique which is used in this study. Median-filtering is another effective technique to suppress or enhance selected events. It is well suited and widely used in corridor stack processing. The separation methods use slopes to distinguish seismic events from each other, where the slope corresponds to velocity on an f-k or a t-x plot. The wavefield separation is first tried on the ZVSP data. The f-k spectra of the total waves and the up going waves after the f-k filtering are shown in Figure 11. The raw ZVSP gather the up-going waves and the down-going waves of the ZVSP data are shown in Figure 12.

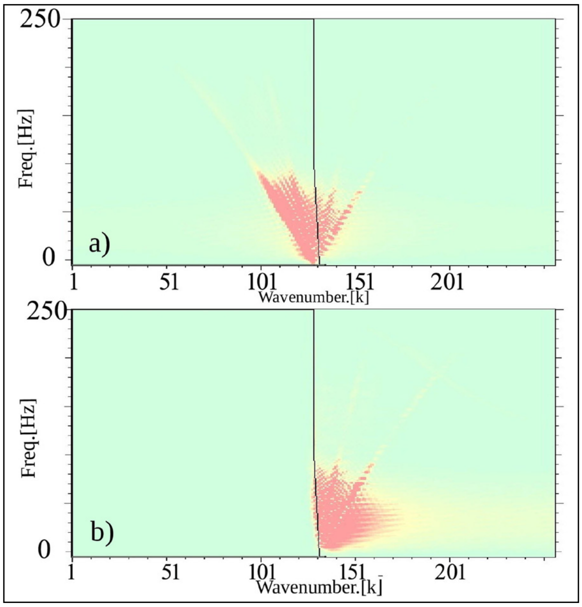

Figure 11- F-k filtering of Z_oVSP data; a) f-k spectrum of the raw gather, b) f-k spectrum after the down-going waves are removed.

After examining the f-k separation procedure and its results on the ZVSP data, the f-k filtering is then applied to all shot gathers. Every fifth gather with 500 m source offset increment is shown in Figure 13 as the raw gathers (a), up-going waves (b), and down-going waves (c), respectively. The zero-offset gather is in the middle indicated by the arrow. As the source offset increases, the wavefield separation becomes more challenging because the up-going and down-going waves behave non-uniformly since the first arrivals and the reflections may travel more horizontally. Wavefield separation may not even be applied beyond some source offsets depending on the data as well as the geometry of the WVSP survey because there is always a danger of removing reflections while attempting to eliminate the down-going waves.

5.3. Spectral Analysis

Frequency or amplitude spectral analysis is performed on both surface seismic and the WVSP data sets. The maximum frequency of 50 Hz and dominant frequency of 25 Hz are seen on the amplitude spectrum plots. For shot S_{15}, the gathers and their f-x spectra are shown in Figure 14. F-x spectra are useful for examining amplitude distributions as well as their

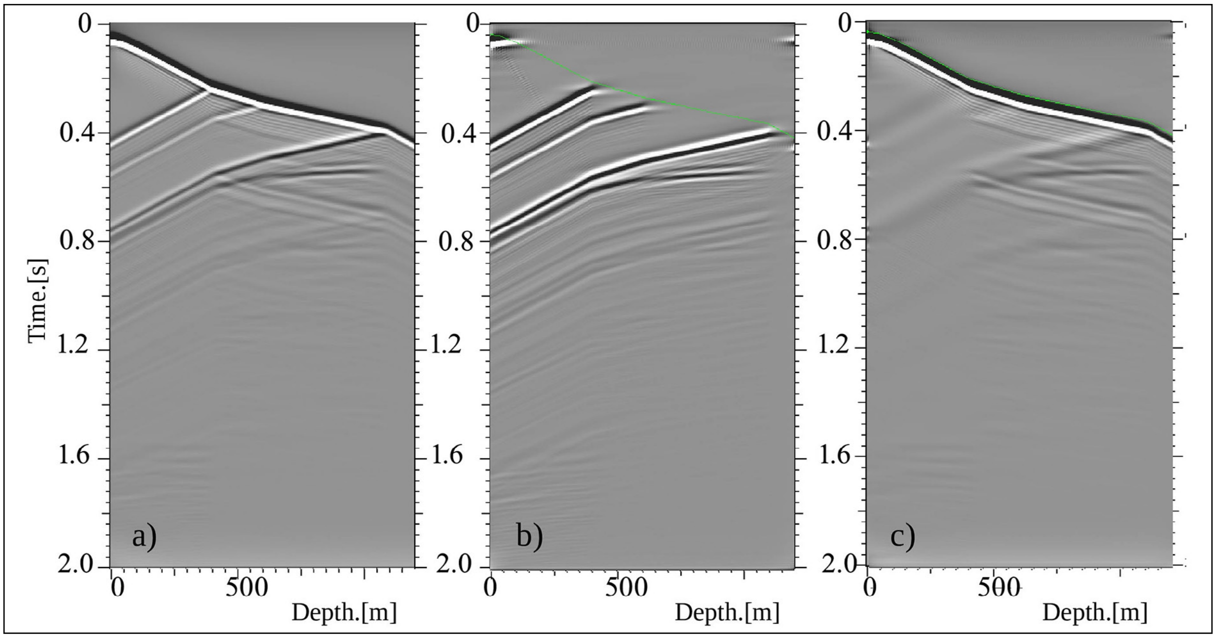

Figure 12- F-k filtering of Z_oVSP shot gather; a) raw data, b) up going waves after separation, c) downgoing waves after separation.

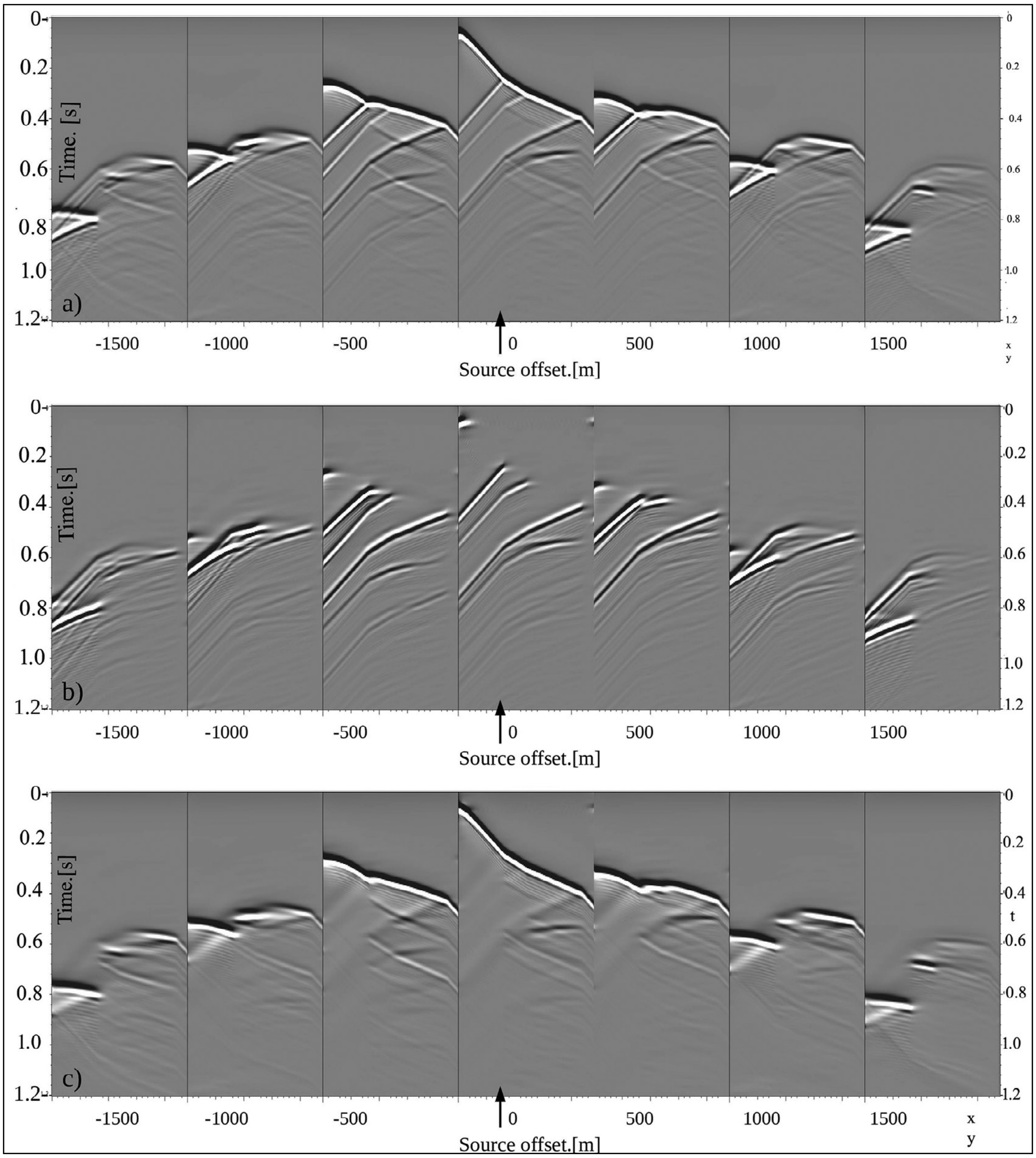

Figure 13- Selected shot gathers of the WVSP data. The arrow indicates the ZVSP gather; a) raw data, b) up-going waves, c) down-going waves after wavefield separation.

frequency content across all traces within a gather. As seen in the figure, high amplitudes are seen on the traces near the source, the amplitudes then become weaker as the distance from the source increases.

5.4. Band-Pass Filtering

An amplitude analysis shows that the data contain low-frequency noise below 5 Hz which is thought to have been created by the modeling program. The noise is removed from the data using an Ormsby band-pass filter. The filtering results are shown as amplitude spectra in Figure 15, where Figure 15a is the average amplitude spectrum from the whole gather, b) from the individual traces in the gather plotted all together, c) from a single trace and d) from the single trace after the filter is applied. The effect of the filtering is shown also on the source gather S_{15} in Figure 16 as a) the raw gather, b) the filtered gather, and c) what is removed by the filter. Since the noise removed section shows no signs of coherent events, the filtering is accepted accurately. The band-pass filtering was then applied to all data.

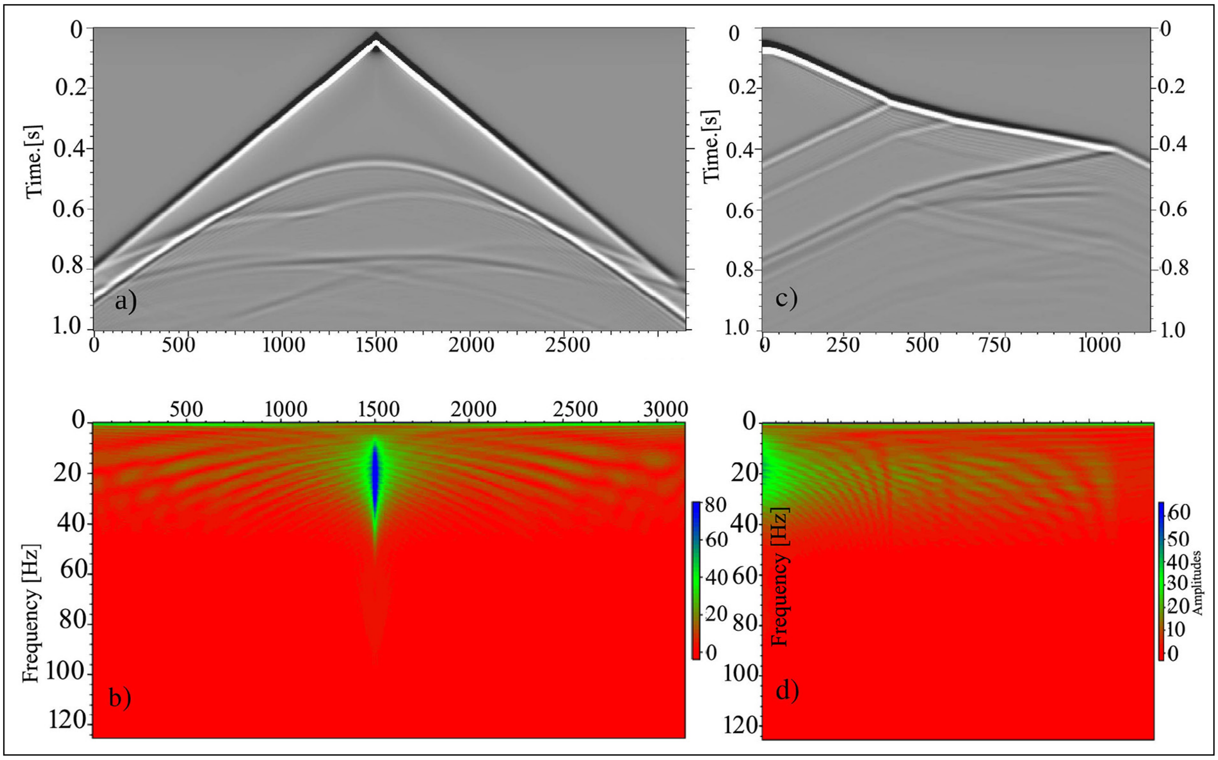

Figure 14- Shot S15 at the borehole location; a) surface seismic gather, b) its f-x spectrum, c) VSP gather, d) its f-x spectrum. The maximum frequency is 50 Hz.

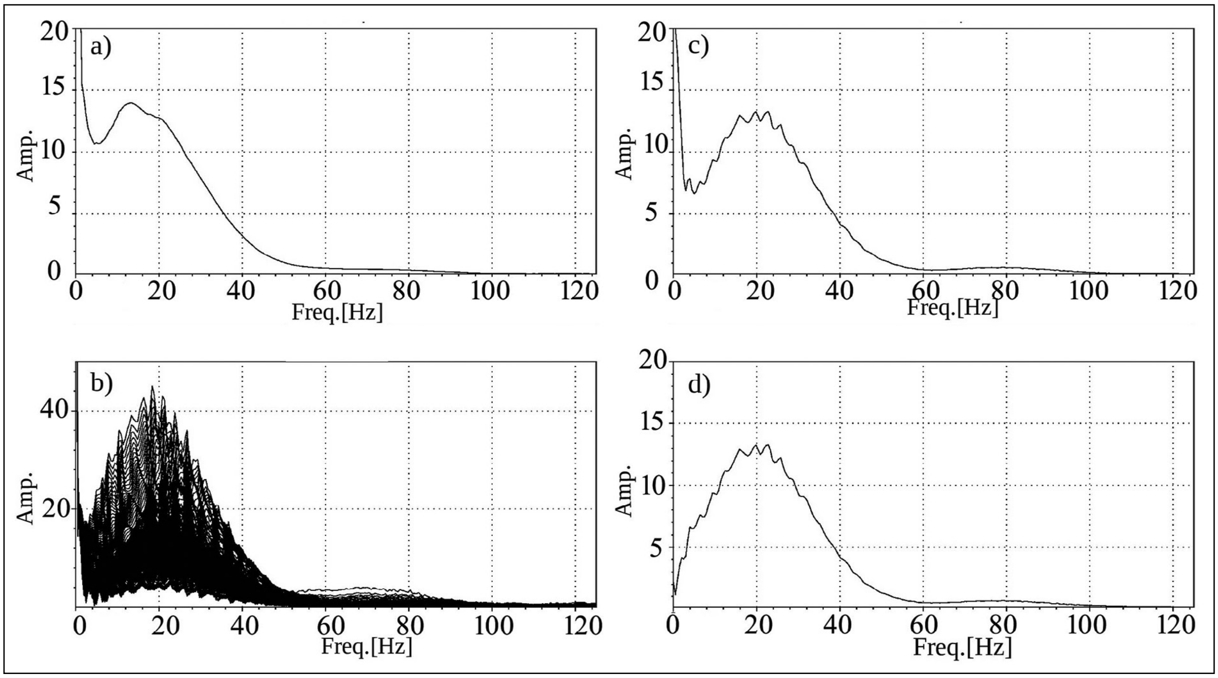

Figure 15- Amplitude spectra of the VSP gather; a) averaged representation, b) from individual traces, c) from a single trace, d) single trace after band-pass filtering applied.

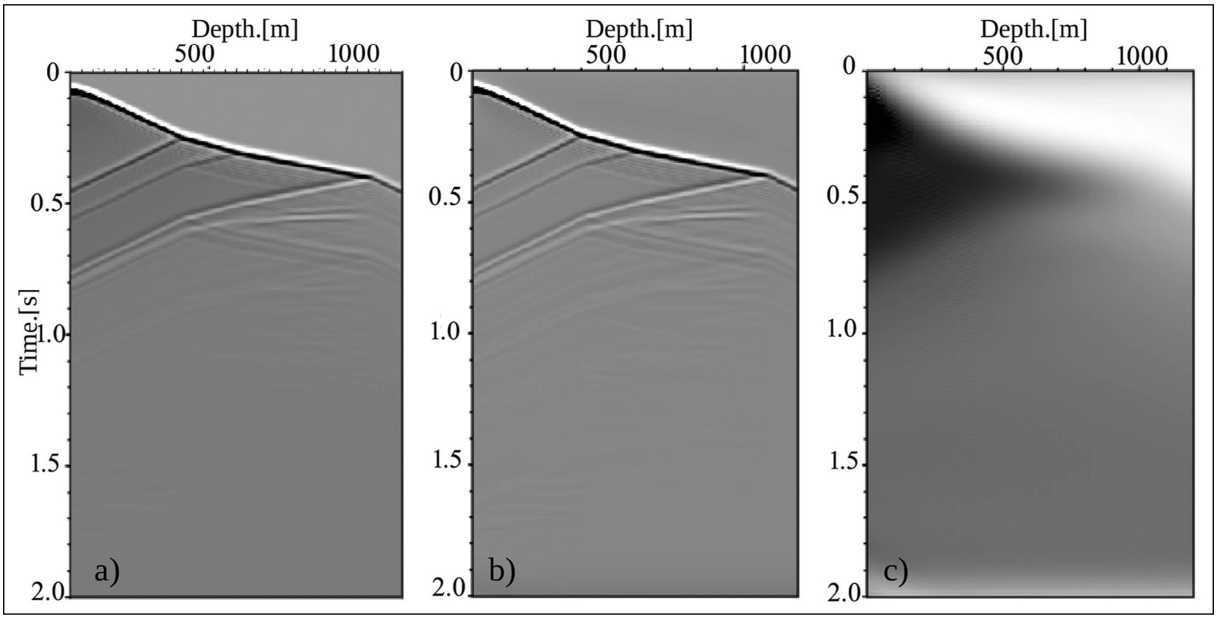

Figure 16- Band-pass filtering, a) raw gather, b) filtered gather, c) what is removed by the filter.

6. CRG Displays

Once the processing is done on the shot gathers, the data are next sorted into CRG for further QC and display. A CRG is a dataset composed of traces from all sources gathered and plotted for a given receiver. When the VSP receiver is at the surface, the CRG gather is equivalent to the surface seismic receiver gather at the same receiver location. Since the receivers are located at different depths in the borehole the CRGs behave differently for different receivers even though the sources do not move. A deeper receiver cannot contain reflection data from the layers above itself however it might still record interval multiples originated by the layers above. It is another look at the data, a CRG representation is useful to view the effects of the processing parameters applied in the shot domain.

Every 40th receiver gather of the WVSP data is shown in Figure 17 as the raw gathers, up going waves and down going waves after mute is applied to remove refractions prior to migration. Further adjustment of the muting process can be done in this domain as well. The changes in the gathers as the depth of the receivers increase can be observed.

7. Velocity Field

The velocity field is an important input in the seismic data migration process. An incorrect velocity field will cause an inaccurate calculation of the travel times. Since inaccurate travel times will result in the migration algorithm selecting the wrong portion of the seismic data for imaging, it will likely result in inaccurate images of the subsurface.

7.1. How to QC Velocity Field before Migration

In this study, the velocity field is assumed known, which is similar to an actual field case where the velocity field is usually derived from the surface seismic and is provided to the VSP processor. The approach to QC the velocity file here is performed as first the first break arrival times for given source-receiver geometry is calculated by using the velocity file, then the calculated times are overlaid on the VSP data to verify that they match. An adequate similarity between the observed data and the calculated travel times are observed in the calculations.

A contour plot of the first break times for zero-offset source (S_{15}) is shown in Figure 18, and the calculated first break times are plotted on the data in Figure 19. It is seen in Figure 19a that the data and the calculated times match overall very well in slopes but the data are delayed by about 45 msec. The time delay is attributed to a delay in the source waveform since the waveform used in the modeling is causal (non-zero-phase, see Figure 3). The data were thus corrected to agree with the calculated travel times to ensure an accurate migration (Figure 19b).

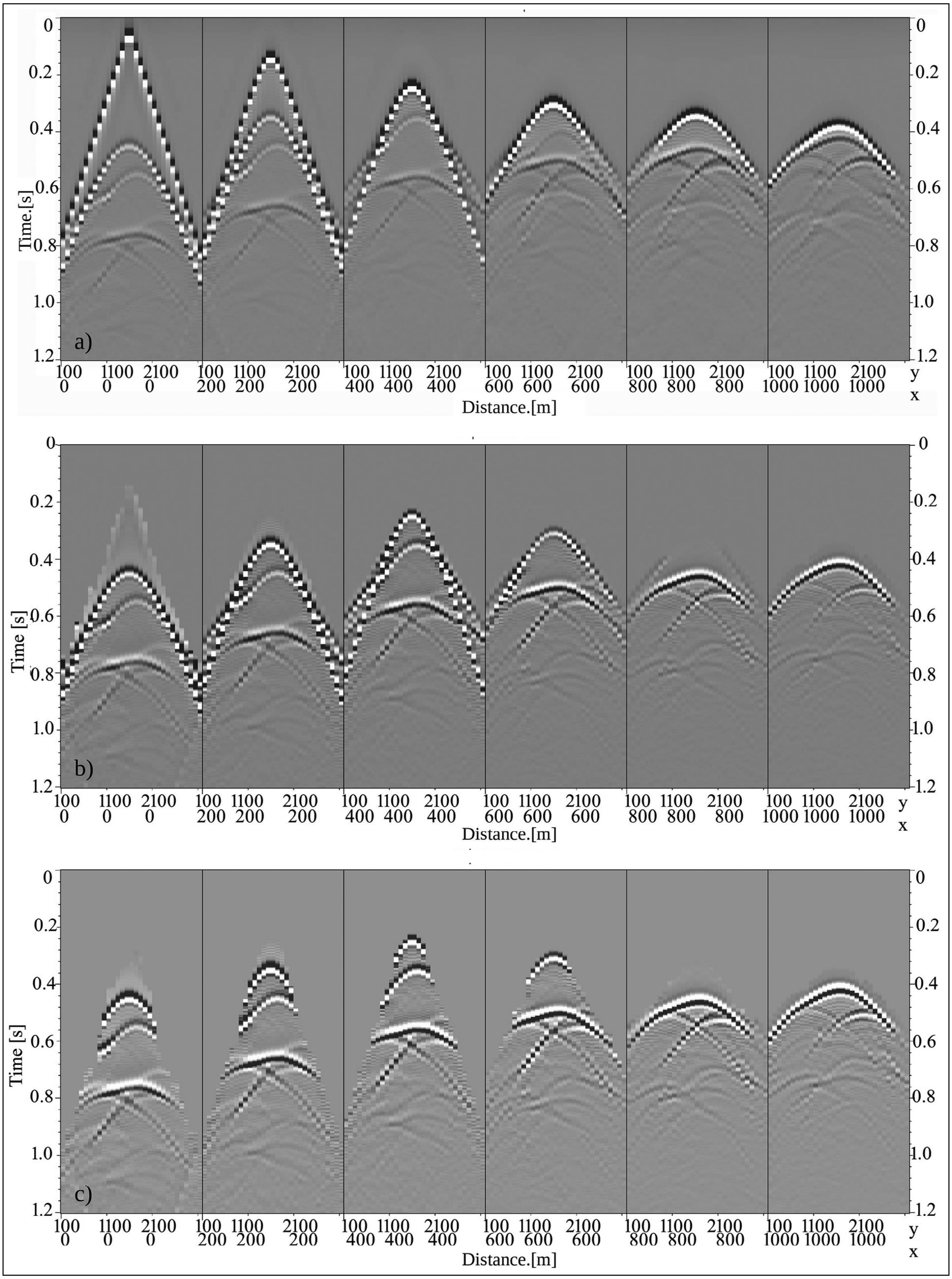

Figure 17- CRG displays of the WVSP data. Every 40th receiver gather is plotted. Receiver depth increases towards the right. Horizontal labels are top is source locations (y), the bottom is receiver depth (x). a) Total waves, b) up going waves after the f-k filtering, c) up going waves after refractions are muted. It is seen in four left panels that some reflections are also removed at the far end offsets.

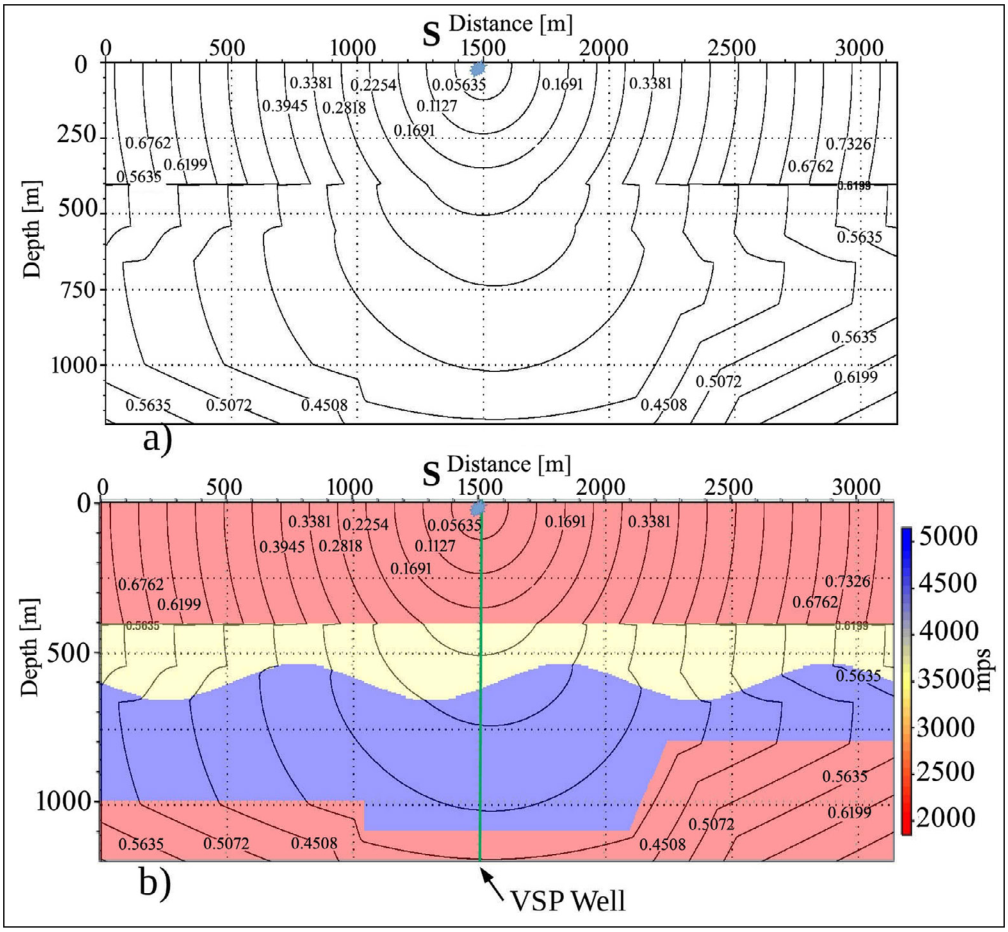

Figure 18- First break travel times from source S15 are plotted; a) as contours, b) on the model together with the well.

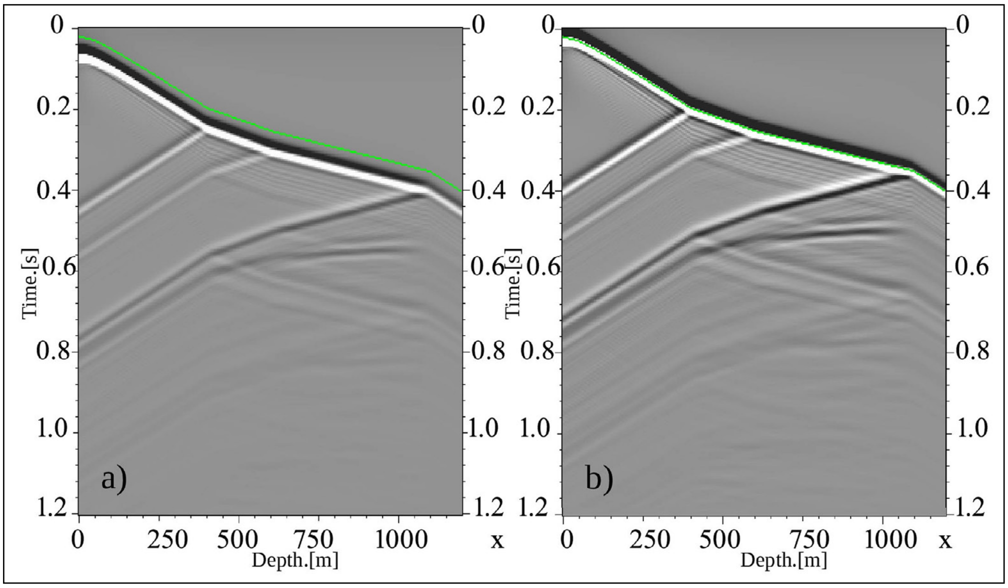

Figure 19- Velocity QC; a) calculated first break times are overlaid on the gather (green line), b) the data is centered on the first break times.

The travel times were calculated for every source. A selection of gathers with posted first break times (green curves) was previously shown in Figure 8 where the visual inspection indicated that the match between the calculated travel times and the data is good, even on the far offset gathers. This QC step proved that the velocity field is accurate and the ray tracing has been performed correctly. The travel time contours of four other source locations are also shown in Figure 20 where the S represents the source location. How the events in a VSP gather are related to the model are explained in Figure 21 where the model, the VSP gather plotted in-depth orientation, and a schematic which displays first breaks, as well as reflections from the layers, are illustrated. After migration, the reflections should land on the layer boundaries.

8. Migration and Imaging and Interpretation of Findings

A hybrid reverse time migration (hRTM) algorithm is used to migrate the WVSP data. The migration code was developed at the Colorado School of Mines (CSM) Geophysics Department, (Hofland, 1990;

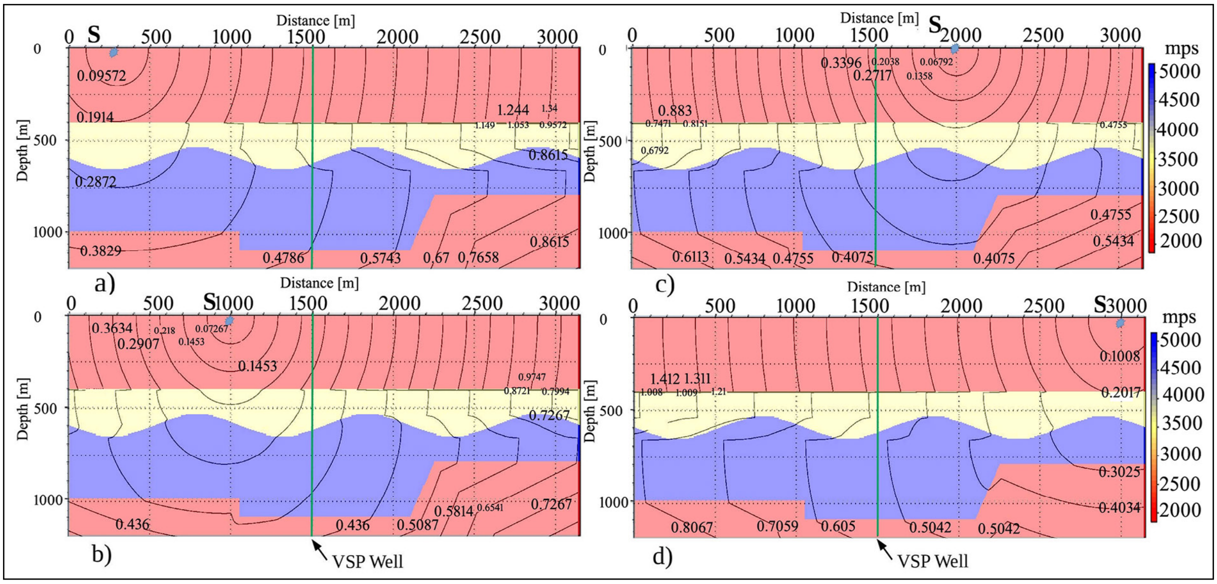

Figure 20- First arrival travel time contours from different source locations, plotted on the model. S is the source. These travel timetables are used in migration.

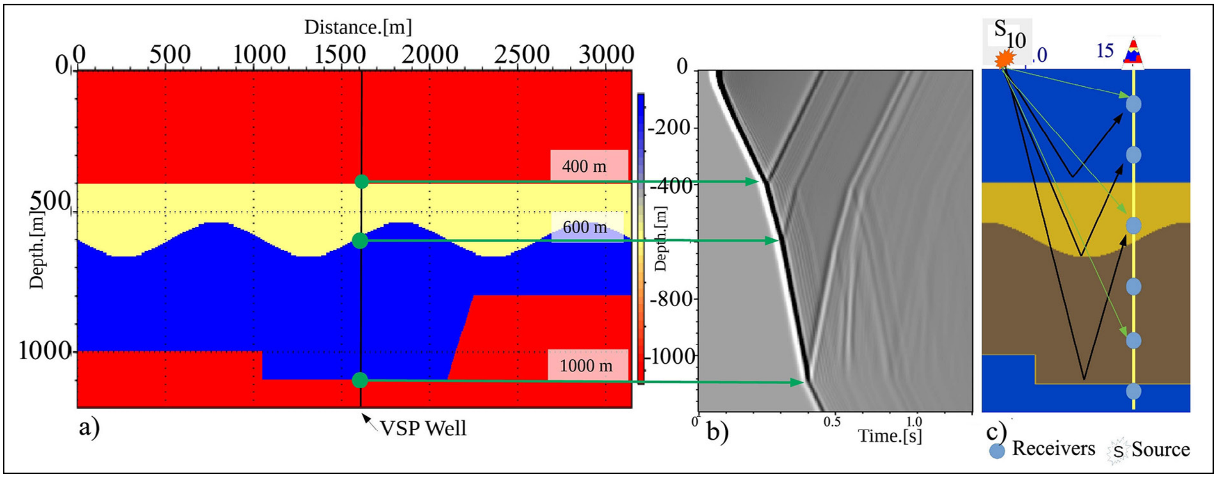

Figure 21- Relationship between the model and the ZVSP gather. The reflections in the ZVSP shot gather are tied to the layers of the model (green arrows); where a) is the model, b) the shot gather, c) is a schematic showing the first arrivals (green) and the reflections (black).

Schneider et al., 1992). It was updated and put into use in the Ubuntu Linux environment by the author. The algorithm consists of four main parts; a) forward travel times are calculated via ray-tracing, b) data is back propagated using a fourth-order space and second-order time solution to the wave equation using the finite differencing method, c) an imaging condition is applied where the forward times coincide with the backward propagation times, and image panels at the propagation times are gathered, and d) the image panels are summed to create a final image panel for the given shot gather.

Each shot gather is migrated separately, the migration process yielded a total of 31 migrated sections. The images are summed together to form a final image using a simple summing procedure. After reviewing individual shot images it is observed that the shallower layers are better illuminated in the near shot offset sections, which is thought to be due to less contamination of events caused by the swings of the tails of the longer source offsets, on the other hand, the deeper layers are better imaged in the longer offsets due to better ray path coverages.

Because the receivers are located at different depths below the surface, more rays impinge in the vicinity of the borehole resulting in unevenly distributed ray paths for VSP geometry. This causes an amplitude build-up near the well, which is also observed in our images. The amplitude build-up becomes more severe on the deeper layers since sources from larger offsets contribute more to these layers. The amplitudes however quickly decay laterally as the image moves away from the well. This sudden variation in the amplitudes needs to be compensated in order to prevent amplitude undulations in the VSP images.

The stacked image obtained from all sources is shown in Figure 22a and its comparison with the model in Figure 22b. The comparison plot indicates that the layers are imaged at their correct locations. At the bottom layer, which was of the main interest in this work, the section around the well and the steeply dipping layer on the right side, and the vertical layer on the left are imaged clearly without any ambiguity. The left dipping middle layer is imaged at its correct location but the image is not as focused as the bottom layer, it loses strength on the down-dip side due to lack of ray path coverage there, the up-dip side is more focused but falls short in length because the layer reaches its turning over point. The first layer is imaged at its correct depth, and overall the image is acceptable, however, it is not well balanced on both sides of the borehole as expected. It seems that the image is truncated on the right side which is because the muting process had removed some of the right-sided reflections earlier than the left-sided ones contributing to the asymmetry of the image. This interpretation is similar to the CRG displays after muting shown in Figure 17c where it is seen in the first three panels that the first reflections are muted unevenly showing asymmetry. As seen in Figure 22a, some artifacts also exist in the image. The artifacts are more severe in the first layer and also below the bottom layer. The circular events are explained as migration artifacts such that not enough cancellation happens during the imaging to suppress the circular, migration sweep events. The artifacts below the bottom layer are due to internal or interbed multiples recorded in the WVSP data.

In order to further explain the circular events, a test is done by creating a stacked image from another data set with a 50 m source interval, which is the half distance of the source interval of the original data; the stacked image is shown in Figure 23. It seems that most of the circular events are eliminated at 50 m source intervals, agreeing with the explanation stated above. The artifacts below the bottom layer are still there, however.

9. Combining Images

In order to illustrate how the images from the two seismic techniques complement each other, the final images of the WVSP and the surface seismic are combined together. A weighted sum approach is used for proper summing to compensate for amplitude differences between the sections, the combined image is shown in Figure 24a. The match between the two sections appears good. As seen in the figure, the WVSP did contribute to surface seismic by infilling the non-coverage parts of the surface seismic, resulting in a more continuous image of the bottom layer. The vertical layer (or a fault) on the left and the dipping layer on the right of the borehole are clearly imaged without any ambiguity. The images of the top and middle layers of the WVSP also match those of the surface seismic near the borehole. The combined image is compared with the model for further QC and shown in Figure 24b, where a good match is seen.

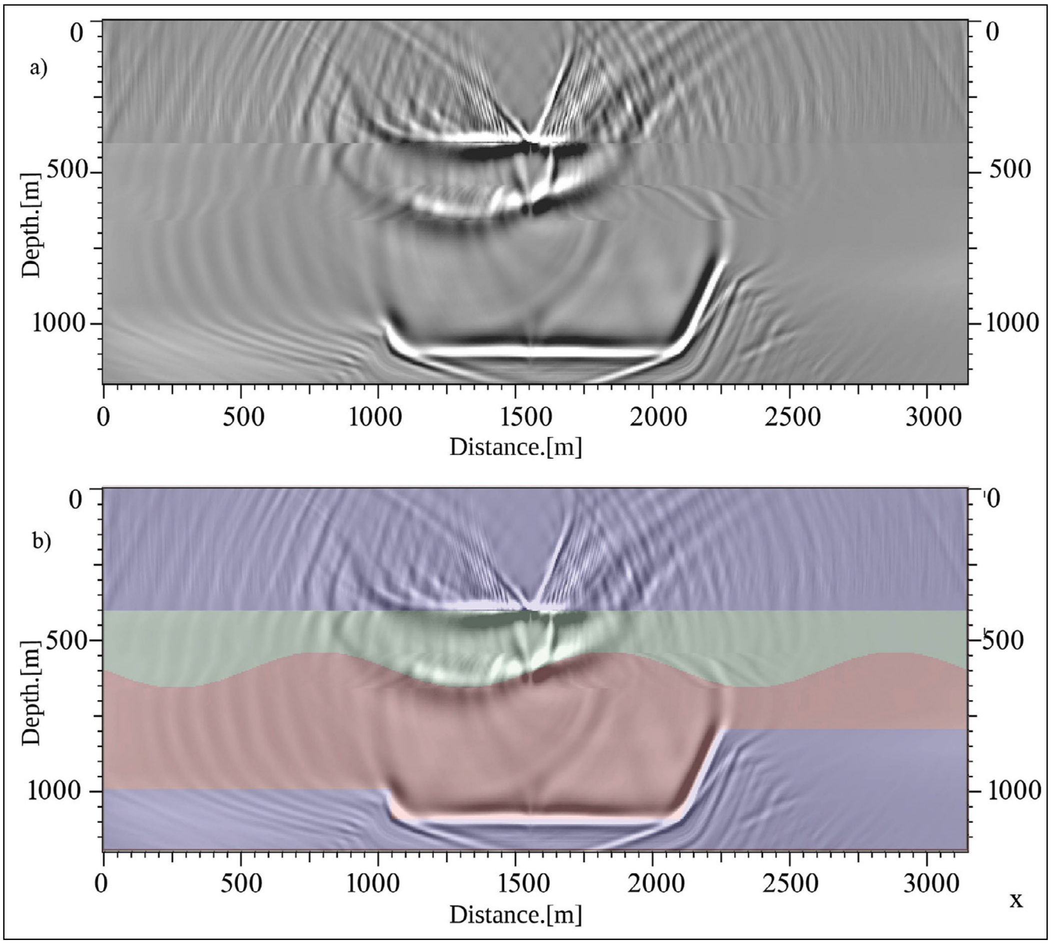

Figure 22- a) Stacked final image obtained after combining all migrated sections. Shot spacing is 100 m. b) final image is overlaid with the model. The match between the image and the model is judged to have been well achieved.

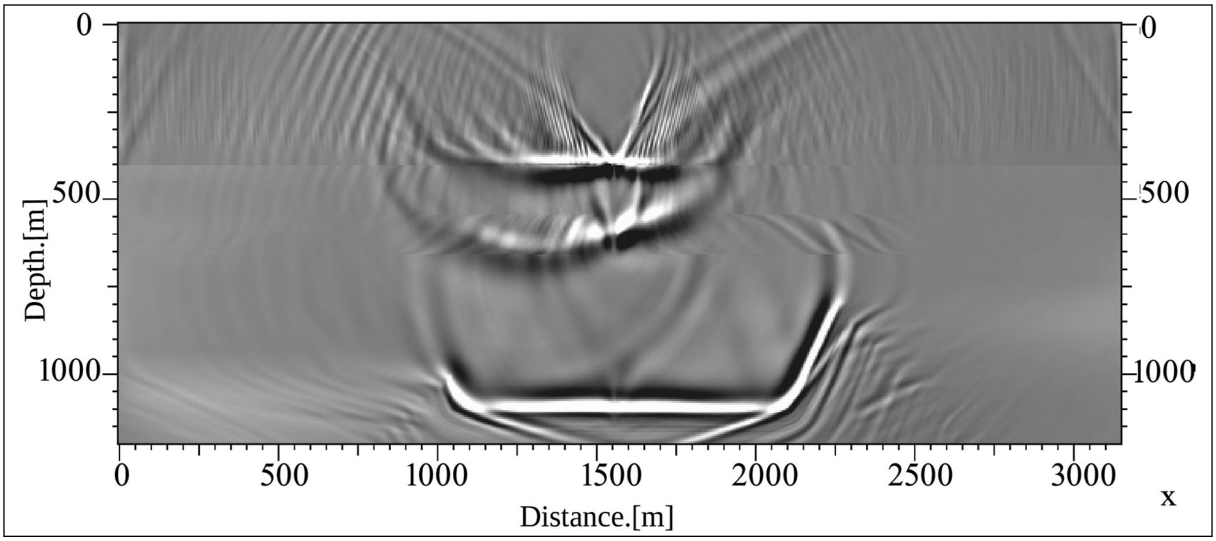

Figure 23- Stacked image from data with 50 m shot spacing. Image quality is increased but the input data volume is doubled.

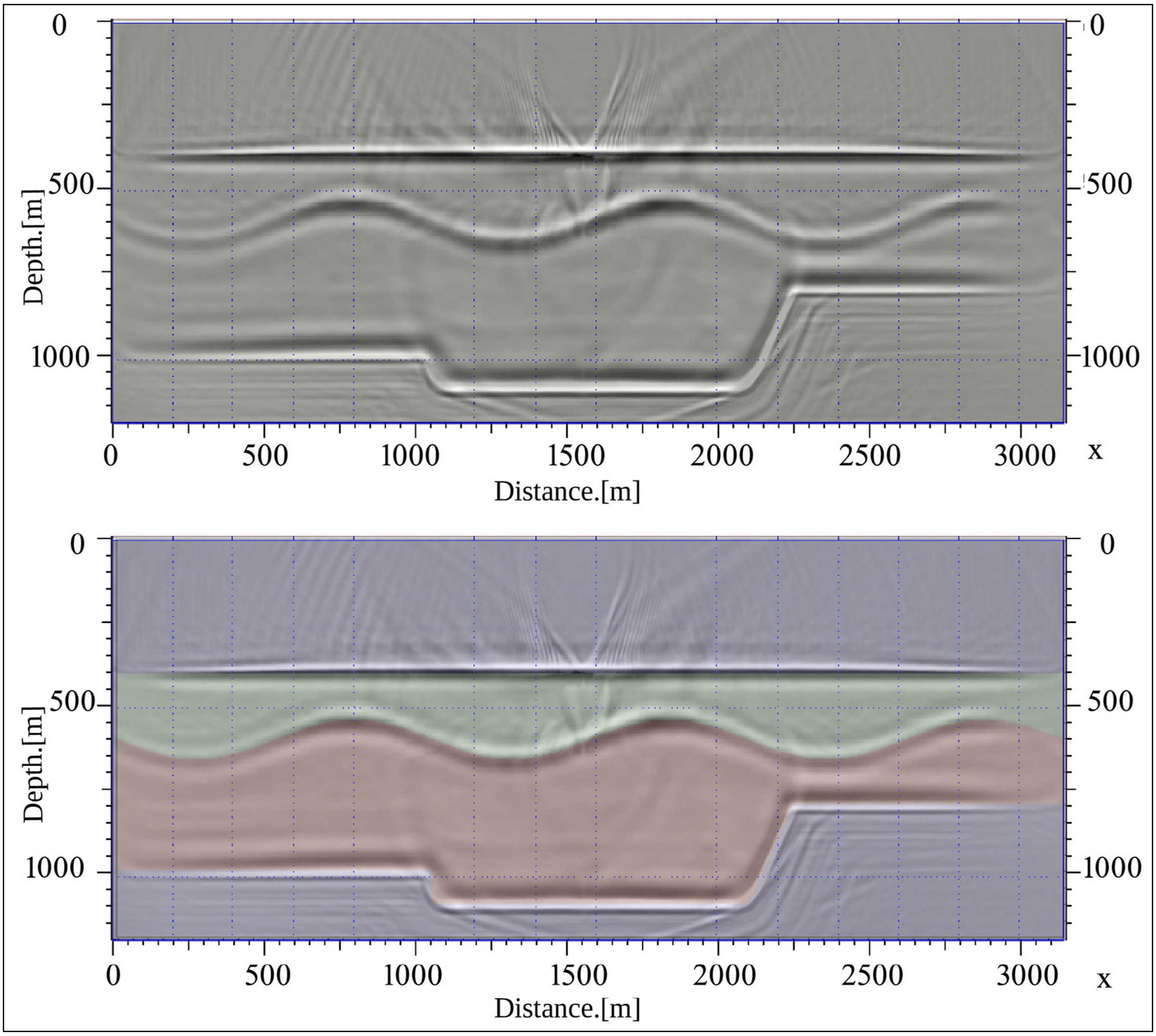

Figure 24- a) Image after combining the WVSP and surface seismic images, b) the image is overlaid with the model.

10. Results

This study shows that a WVSP survey is an effective, valid, and useful tool to record seismic events in areas where a surface seismic survey might have difficulty capturing reflected rays. These areas may be labelled as shadow zones for surface seismic and may be characterized as layers with steep dips, fault faces, near-vertical structures, or graben-like structures as shown in this study. Successful migration of the reflections recorded on a WVSP survey from those seismically problematic areas may lead to the construction of more useful images of the subsurface.

It is shown here that the WVSP survey successfully imaged the layers with steep dips facing the borehole at the bottom layer on the model. The undulating middle layer is imaged fine around the borehole. The WVSP image tied the image from the surface seismic well.

The combined image produced a more complete final image of the model. The layers of the surface seismic and WVSP matched each other around the borehole. The parts missing in the image derived from the surface seismic are accurately recovered by the WVSP removing ambiguities in the images obtained from the surface seismic alone. The combined image has shown that the WVSP contributed and completed surface seismic for a more accurate representation of the subsurface, however, the WVSP produced and introduced more coherent noise and artifacts that were not seen in the surface seismic image.

In many seismic exploration studies, a VSP is routinely acquired and processed to help surface seismic for interpretation purposes. Since WVSP is from a different geometry and from a different data set that is independent of surface seismic, it does provide a second look at the subsurface at least around the VSP well. Also, because VSP data might be of higher frequency than surface seismic, it may also be used to help delineate and reveal subsurface structures such as buried small faults, river bed channels, sand pockets, and reservoir properties which may be harder to detect on surface seismic data alone.

WVSP data can be acquired together with surface seismic using surface seismic sources provided there is a borehole available in the survey area.

Acknowledgements

I would like to thank the Colorado School of Mines Geophysics Department for providing the Seismic UNIX (SU) package to the Geophysical Community. I greatly appreciate and fondly remember my graduate advisor, Prof. Dr. Alfred H. BALCH, and his Borehole Seismic Group, for their efforts and support of the development of the WVSP imaging package. I thank Paul GAROSSINO and Joe WADE for their personal help for the use of some of their codes, I thank Dr. Fethi Ahmet YUKSEL of I. U. for his encouragement, discussions, and endless geophysical support in the publication of this work. I also thank Cahit DÖNMEZ of MTA for his guidance and discussions about the subjects in this paper. I thank Bruce E. CORNISH for his help in editing this paper and for his continued support through geophysical discussions.

References

Balch, A. H., Lee, M. W. 1984. Vertical Seismic Profiling: Technique, Applications, and Case Histories. International Human Resource Development Corporation, Boston, MA, 488.

Çınar, H. 1989. VSP verileriyle kayaçların soğurma özelliklerinin belirlenmesi. Yüksek Lisans Tezi, Karadeniz Teknik Üniversitesi, Jeofizik Bölümü, Trabzon, Türkiye.

Erdemir, C. 2018. Survey design for 2D seismic imaging exercise. İstanbul Yerbilimleri Dergisi 28 (1-2), 71-92.

Galperin, E. I. 1985. Vertical Seismic Profiling and Its Exploration Potential. Springer Science and Business Media.

Hardage, B. A. 1985. Vertical seismic profiling, part a: principles. The Journal of the Acoustical Society of America 78, 282.

Hofland, G. S. 1990. Multi-mode, multiple offset VSP reverse time migration (imaging) of a complex, physical Earth model. Master Thesis, Colorado School of Mines, Golden, Colorado, United States (unpublished).

Hornby, B. E., Yu, J., Sharp, J. A., Ray, A., Quist, Y. 2006. VSP - beyond time to depth. 2nd European Association Geoscientists and Engineers St. Petersburg International Conference and Exhibition on Geosciences, October.

Jaramillo, H. 1993. Modeling and imaging of computational and physical VSP data. Master Thesis, Colorado School of Mines, Golden, CO, United States (unpublished).

Jaramillo, H. H., Balch, A. H., Erdemir, C., Rousseau, J. P. 1993. Multimode reverse time VSP imaging over complex structures at Yucca Mountain, Nye County, Nevada, International Nuclear Information System (INIS), USA.

Karslı, H. 1995. Soğurucu tabakalı ortamlarda yapay düşey sismik profili sismogramlarının hesaplanması. Yüksek Lisans Tezi, Karadeniz Teknik Üniversitesi, Jeofizik Mühendisliği, Trabzon, Türkiye.

Ray, A., Quist, Y., Yu, Z., Sugianto, H., Hornby, B. 2005. Acquisition of 2D walkaway VSP data to provide improved imaging of the Thunder Horse North field, Gulf of Mexico. The Leading Edge, Special section Offshore, Apr 2005, Seg, 2005-0476. SEG, 2005-SEG Annual Meeting, 06-11 November, Houston, TX, USA.

Ray, A., Quist, Y., Yu, Z., Sugianto, H., Hornby, B. 2005. Acquisition of 2D walkaway VSP data to provide improved imaging of the Thunder Horse North field, Gulf of Mexico. The Leading Edge, 430-432.

Schneider, W. A. J., Ranzinger, K., Balch, A., Kruse, C. 1992. A dynamic programming approach to first arrival traveltime computation in media with arbitrarily distributed velocities. Geophysics 57, 39–50.

Seismic Velocities. https://gpg.geosci.xyz/content/physical_properties/seismic_velocity_duplicate.html. 21 December 2021.

Stockwell, J. W., Cohen, J. K. 2008. The New SU User's Manual, Version 4.0. The Seismic Unix Project, Center for Wave Phenomena (CWP), Colorado School of Mines.

Toksöz, M. N., Stewart R. R. 1985. Vertical seismic profiling, part b, advanced concepts. The Journal of the Acoustical Society of America 78, 282.

Wyatt, K. D. 1987. Vertical seismic profiling. The Journal of the Acoustical Society of America 82, 2165.

Yılmaz, M. 2015. Düşey sismik profil (VSP) verisinin üç boyutlu (3D) yüzey sismiği ile karşılaştırılması. Yüksek Lisans Tezi, Süleyman Demirel Üniversitesi, Fen Bilimleri Enstitüsü, Jeofizik Mühendisliği Anabilim Dalı, Isparta, Türkiye.

Yilmaz, O. 1987. Seismic Data Processing. Society of Exploration Geophysicists, 526.